

Meson-baryon scattering to one-loop order in heavy baryon chiral perturbation theory

Bo-Lin Huang ^{*1,2}, Jin-Sheng Zhang^{†1}, Yun-De Li^{‡1}, and Norbert Kaiser^{§2}

¹Department of Physics, Yunnan University, Kunming 650091, China

²Physik Department, Technische Universität München, D-85747 Garching, Germany

January 7, 2019

Abstract

We calculate the T-matrices of pseudoscalar meson octet-baryon scattering to one-loop order in SU(3) heavy baryon chiral perturbation theory. The pertinent combinations of low-energy constants are determined by fitting to phase shifts of πN and KN scattering and the corresponding data. By using these low-energy constants, we predict scattering lengths and phase shifts for other channels and obtain reasonable results. The issue of convergence is discussed in detail.

PACS numbers: 13.75.Jz, 12.39.Fe, 12.38.Bx

Keywords: Chiral perturbation theory, meson-baryon scattering

1 Introduction

As it is well known, quantum chromodynamics (QCD) becomes non-perturbative at low energies, and thus it is very difficult to use perturbative methods to calculate the low-energy hadronic processes. For treating this problem, effective field theory (EFT) is introduced as a substitute to low-energy QCD. The EFT is formulated in terms of the most general Lagrangian consistent with the chiral symmetry of QCD, as well as the other continuous and discrete symmetries. In the EFT, the degrees of freedom are no longer quarks and gluons, but rather hadrons, i.e. pions, kaons, eta-mesons, and baryons. The corresponding field theoretical formalism is called chiral perturbation theory (ChPT) [1, 2]. The heavy baryon chiral perturbation theory (HB χ PT) has been proposed and developed to solve the power-counting problem which arises from the non-vanishing baryon mass in the chiral limit [3, 4]. Although relativistic approaches (such as infrared regularization [5] and the extended on-mass-shell scheme [6, 7]) have lead to some progress in certain aspects [8, 9], HB χ PT is still a reasonable and powerful tool in the study of meson-baryon scattering processes.

Over the years, SU(2) HB χ PT have been widely used to investigate the low-energy processes of pions and nucleons and achieved many successes [10, 11, 12, 13]. For processes involving kaons or hyperons, one has to use three-flavor chiral dynamics. The predictions for meson-baryon scattering lengths in SU(3) HB χ PT have been given in detail and reasonable results have been obtained in Refs. [14, 15, 16, 17, 18]. In a previous paper [19] we have investigated the KN and $\bar{K}N$ scattering to one-loop order in SU(3) HB χ PT by fitting to phase shifts of KN scattering and obtained reasonable results. In this paper, we will extend this approach to predictions of pseudoscalar meson octet-baryon scattering in all channels by fitting to phase shifts of elastic πN and KN scattering simultaneously.

In Sec. 2, the Lagrangians involved in the calculations up to one-loop order are presented in detail. In Sec. 3, we present the T-matrices for the meson-baryon scattering processes order by order and channel by channel. In Sec. 4, we outline how to calculate phase shifts and scattering lengths. Section 5 is devoted to the presentation and discussion of our results and it includes also a brief summary.

*bolin.huang@foxmail.com

†zjs19920501@163.com

‡yndxlyd@163.com

§n.kaiser@ph.tum.de

2 Chiral Lagrangian

Our calculation of the elastic meson-baryon scattering is based on the SU(3) effective chiral Lagrangian in the heavy baryon formulation

$$\mathcal{L} = \mathcal{L}_{\phi\phi} + \mathcal{L}_{\phi B}. \quad (1)$$

The traceless hermitian 3×3 matrices ϕ and B include the pseudoscalar Goldstone boson fields (π, K, \bar{K}, η) and the octet baryons fields (N, Λ, Σ, Ξ), respectively. The lowest-order SU(3) chiral Lagrangians for meson-meson and meson-baryon interaction take the form [20]

$$\mathcal{L}_{\phi\phi}^{(2)} = \frac{f^2}{4} \text{tr}(u_\mu u^\mu + \chi_+), \quad (2)$$

$$\mathcal{L}_{\phi B}^{(1)} = \text{tr}(i\bar{B}[v \cdot D, B]) + D \text{tr}(\bar{B}S_\mu\{u^\mu, B\}) + F \text{tr}(\bar{B}S_\mu[u^\mu, B]), \quad (3)$$

where D_μ denotes the chiral covariant derivative

$$[D_\mu, B] = \partial_\mu B + [\Gamma_\mu, B], \quad (4)$$

and S_μ is the covariant spin-operator. In practice one works with $\vec{\sigma}$ the Pauli spin matrices

$$S^\mu = \left(0, \frac{\vec{\sigma}}{2}\right). \quad (5)$$

The chiral connection $\Gamma^\mu = [\xi^\dagger, \partial^\mu \xi]/2$ and the axial vector quantity $u^\mu = i\{\xi^\dagger, \partial^\mu \xi\}$ contain an even and odd number of meson fields, respectively. The SU(3) matrix $U = \xi^2 = \exp(i\phi/f)$ collect the pseudoscalar Goldstone boson fields. The parameter f is the pseudoscalar decay constant in the chiral limit. The axial vector coupling constants D and F can be determined by fitting the semi-leptonic decays ($D \simeq 0.8, F \simeq 0.5$) [21]. The quantity $\chi_+ = \xi^\dagger \chi \xi^\dagger + \xi \chi \xi$ with $\chi = \text{diag}(m_\pi^2, m_\pi^2, 2m_K^2 - m_\pi^2)$ introduces explicit chiral symmetry breaking terms. The complete heavy-baryon Lagrangian at next-to-leading order splits up into two parts

$$\mathcal{L}_{\phi B}^{(2)} = \mathcal{L}_{\phi B}^{(2,1/M_0)} + \mathcal{L}_{\phi B}^{(2,\text{ct})}, \quad (6)$$

where $\mathcal{L}_{\phi B}^{(2,1/M_0)}$ denotes $1/M_0$ corrections of dimension two with fixed coefficients and it stems from the $1/M_0$ expansion of the original relativistic leading-order Lagrangian $\mathcal{L}_{\phi B}^{(1)}$ [20]. The pertinent terms read

$$\begin{aligned} \mathcal{L}_{\phi B}^{(2,1/M_0)} = & \frac{D^2 - 3F^2}{24M_0} \text{tr}(\bar{B}[v \cdot u, [v \cdot u, B]]) - \frac{D^2}{12M_0} \text{tr}(\bar{B}B) \text{tr}(v \cdot u v \cdot u) \\ & - \frac{DF}{4M_0} \text{tr}(\bar{B}[v \cdot u, \{v \cdot u, B\}]) - \frac{1}{2M_0} \text{tr}(\bar{B}[D_\mu, [D^\mu, B]]) \\ & + \frac{1}{2M_0} \text{tr}(\bar{B}[v \cdot D, [v \cdot D, B]]) - \frac{iD}{2M_0} \text{tr}(\bar{B}S_\mu[D^\mu, \{v \cdot u, B\}]) \\ & - \frac{iF}{2M_0} \text{tr}(\bar{B}S_\mu[D^\mu, [v \cdot u, B]]) - \frac{iF}{2M_0} \text{tr}(\bar{B}S_\mu[v \cdot u, [D^\mu, B]]) \\ & - \frac{iD}{2M_0} \text{tr}(\bar{B}S_\mu\{v \cdot u, [D^\mu, B]\}), \end{aligned} \quad (7)$$

where M_0 denotes the baryon mass in the chiral limit. The remaining meson-baryon Lagrangian $\mathcal{L}_{\phi B}^{(2,\text{ct})}$ involves new low-energy constants (LECs) and it can be obtained from the relativistic Lagrangian in Ref. [22]. The pertinent interaction terms read

$$\begin{aligned} \mathcal{L}_{\phi B}^{(2,\text{ct})} = & b_D \text{tr}(\bar{B}\{\chi_+, B\}) + b_F \text{tr}(\bar{B}[\chi_+, B]) + b_0 \text{tr}(\bar{B}B) \text{tr}(\chi_+) + b_1 \text{tr}(\bar{B}\{u^\mu u_\mu, B\}) \\ & + b_2 \text{tr}(\bar{B}[u^\mu u_\mu, B]) + b_3 \text{tr}(\bar{B}B) \text{tr}(u^\mu u_\mu) + b_4 \text{tr}(\bar{B}u^\mu) \text{tr}(u_\mu B) + b_5 \text{tr}(\bar{B}\{v \cdot u v \cdot u, B\}) \\ & + b_6 \text{tr}(\bar{B}[v \cdot u v \cdot u, B]) + b_7 \text{tr}(\bar{B}B) \text{tr}(v \cdot u v \cdot u) + b_8 \text{tr}(\bar{B}v \cdot u) \text{tr}(v \cdot u B) \\ & + b_9 \text{tr}(\bar{B}\{[u^\mu, u^\nu], [S_\mu, S_\nu] B\}) + b_{10} \text{tr}(\bar{B}[[u^\mu, u^\nu], [S_\mu, S_\nu] B]) \\ & + b_{11} \text{tr}(\bar{B}u^\mu) \text{tr}(u^\nu [S_\mu, S_\nu] B). \end{aligned} \quad (8)$$

The first three terms proportional to the LECs $b_{D,F,0}$ give rise to explicit chiral symmetry breaking. Note that all LECs b_i have dimension mass⁻¹.

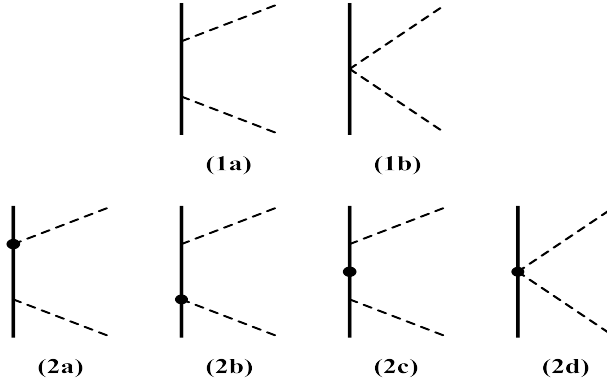


Figure 1: Tree diagrams contributing at first and second chiral order. Dashed lines represent Goldstone bosons and solid lines represent octet baryons. The heavy dots refer to vertices from $\mathcal{L}_{\phi B}^{(2)}$. Diagrams with crossed meson lines are not shown.

3 T-matrices for meson-baryon scattering

We are considering in this work only elastic meson-baryon scattering processes $M(\mathbf{q}) + B(-\mathbf{q}) \rightarrow M(\mathbf{q}') + B(-\mathbf{q}')$ in the center-of-mass system with $|\mathbf{q}| = |\mathbf{q}'| = q$. The T-matrix takes the following form:

$$T_{MB}^{(I)} = V_{MB}^{(I)}(q) + i\boldsymbol{\sigma} \cdot (\mathbf{q}' \times \mathbf{q}) W_{MB}^{(I)}(q), \quad (9)$$

where I denotes the total isospin of the meson-baryon system. Furthermore, $V_{MB}^{(I)}(q)$ refers to the non-spin-flip meson-baryon amplitude and $W_{MB}^{(I)}(q)$ refers to the spin-flip meson-baryon amplitude. In the following subsections we calculate the T-matrices order by order for every channel and specify them by giving the pair $T_{MB}^{(I)} = \{V_{MB}^{(I)}, W_{MB}^{(I)}\}$. The velocity four-vector is chosen as $v^\mu = (1, 0, 0, 0)$ throughout this paper.

3.1 Leading order amplitudes

For elastic meson-baryon scatterings, the leading order $\mathcal{O}(q)$ amplitudes resulting from the diagrams (1a) and (1b) in Fig. 1 (and their crossed partners) read:

$$T_{\pi N}^{(3/2)} = \left\{ \frac{-w_\pi^2 + q^2 z(D+F)^2}{2f_\pi^2 w_\pi}, -\frac{(D+F)^2}{2f_\pi^2 w_\pi} \right\}, \quad (10)$$

$$T_{\pi N}^{(1/2)} = \left\{ \frac{w_\pi^2 - q^2 z(D+F)^2}{f_\pi^2 w_\pi}, -\frac{(D+F)^2}{2f_\pi^2 w_\pi} \right\}, \quad (11)$$

$$T_{\pi \Sigma}^{(2)} = \left\{ \frac{-3w_\pi^2 + q^2 z(D^2 + 3F^2)}{3f_\pi^2 w_\pi}, -\frac{D^2 + 3F^2}{3f_\pi^2 w_\pi} \right\}, \quad (12)$$

$$T_{\pi \Sigma}^{(1)} = \left\{ \frac{3w_\pi^2 - q^2 z(D^2 + 3F^2)}{3f_\pi^2 w_\pi}, \frac{D^2 - 9F^2}{3f_\pi^2 w_\pi} \right\}, \quad (13)$$

$$T_{\pi \Sigma}^{(0)} = \left\{ \frac{6w_\pi^2 - 2q^2 z(D^2 + 3F^2)}{3f_\pi^2 w_\pi}, \frac{-4D^2 + 6F^2}{3f_\pi^2 w_\pi} \right\}, \quad (14)$$

$$T_{\pi \Xi}^{(3/2)} = \left\{ \frac{-w_\pi^2 + q^2 z(D-F)^2}{2f_\pi^2 w_\pi}, -\frac{(D-F)^2}{2f_\pi^2 w_\pi} \right\}, \quad (15)$$

$$T_{\pi\Xi}^{(1/2)} = \left\{ \frac{w_\pi^2 - q^2 z(D-F)^2}{f_\pi^2 w_\pi}, -\frac{(D-F)^2}{2f_\pi^2 w_\pi} \right\}, \quad (16)$$

$$T_{\pi\Lambda} = \left\{ 0, -\frac{2D^2}{3f_\pi^2 w_\pi} \right\}, \quad (17)$$

$$T_{KN}^{(1)} = \left\{ \frac{-3w_K^2 + q^2 z(D^2 + 3F^2)}{3f_K^2 w_K}, -\frac{D^2 + 3F^2}{3f_K^2 w_K} \right\}, \quad (18)$$

$$T_{KN}^{(0)} = \left\{ \frac{2q^2 zD(D-3F)}{3f_K^2 w_K}, -\frac{2D(D-3F)}{3f_K^2 w_K} \right\}, \quad (19)$$

$$T_{KN}^{(1)} = \left\{ \frac{w_K^2 - q^2 z(D-F)^2}{2f_K^2 w_K}, -\frac{(D-F)^2}{2f_K^2 w_K} \right\}, \quad (20)$$

$$T_{KN}^{(0)} = \left\{ \frac{9w_K^2 - q^2 z(D+3F)^2}{6f_K^2 w_K}, -\frac{(D+3F)^2}{6f_K^2 w_K} \right\}, \quad (21)$$

$$T_{K\Sigma}^{(3/2)} = \left\{ \frac{-w_K^2 + q^2 z(D+F)^2}{2f_K^2 w_K}, -\frac{(D+F)^2}{2f_K^2 w_K} \right\}, \quad (22)$$

$$T_{K\Sigma}^{(1/2)} = \left\{ \frac{w_K^2 - q^2 z(D^2 - DF + F^2)}{f_K^2 w_K}, -\frac{D^2 - 4DF + F^2}{2f_K^2 w_K} \right\}, \quad (23)$$

$$T_{K\Sigma}^{(3/2)} = \left\{ \frac{-w_K^2 + q^2 z(D-F)^2}{2f_K^2 w_K}, -\frac{(D-F)^2}{2f_K^2 w_K} \right\}, \quad (24)$$

$$T_{K\Sigma}^{(1/2)} = \left\{ \frac{w_K^2 - q^2 z(D^2 + DF + F^2)}{f_K^2 w_K}, -\frac{D^2 + 4DF + F^2}{2f_K^2 w_K} \right\}, \quad (25)$$

$$T_{K\Xi}^{(1)} = \left\{ \frac{w_K^2 - q^2 z(D+F)^2}{2f_K^2 w_K}, -\frac{(D+F)^2}{2f_K^2 w_K} \right\}, \quad (26)$$

$$T_{K\Xi}^{(0)} = \left\{ \frac{9w_K^2 - q^2 z(D-3F)^2}{6f_K^2 w_K}, -\frac{(D-3F)^2}{6f_K^2 w_K} \right\}, \quad (27)$$

$$T_{K\Xi}^{(1)} = \left\{ \frac{-3w_K^2 + q^2 z(D^2 + 3F^2)}{3f_K^2 w_K}, -\frac{D^2 + 3F^2}{3f_K^2 w_K} \right\}, \quad (28)$$

$$T_{K\Xi}^{(0)} = \left\{ \frac{2q^2 zD(D+3F)}{3f_K^2 w_K}, -\frac{2D(D+3F)}{3f_K^2 w_K} \right\}, \quad (29)$$

$$T_{K\Lambda} = \left\{ -\frac{q^2 zDF}{f_K^2 w_K}, -\frac{D^2 + 9F^2}{6f_K^2 w_K} \right\}, \quad (30)$$

$$T_{\bar{K}\Lambda} = \left\{ \frac{q^2 z DF}{f_K^2 w_K}, -\frac{D^2 + 9F^2}{6f_K^2 w_K} \right\}, \quad (31)$$

$$T_{\eta N} = \left\{ 0, -\frac{(D - 3F)^2}{6f_\eta^2 w_\eta} \right\}, \quad (32)$$

$$T_{\eta\Sigma} = \left\{ 0, -\frac{2D^2}{3f_\eta^2 w_\eta} \right\}, \quad (33)$$

$$T_{\eta\Xi} = \left\{ 0, -\frac{(D + 3F)^2}{6f_\eta^2 w_\eta} \right\}, \quad (34)$$

$$T_{\eta\Lambda} = \left\{ 0, -\frac{2D^2}{3f_\eta^2 w_\eta} \right\}, \quad (35)$$

where $w_{\pi,K,\eta} = (m_{\pi,K,\eta}^2 + q^2)^{1/2}$ denotes the center-of-mass energy of the pion, kaon and eta, respectively, and $z = \cos(\theta)$ is the cosine of the angle between \mathbf{q} and \mathbf{q}' . We take the renormalized (physical) decay constants $f_{\pi,K,\eta}$ instead of f (the chiral limit value). Note that, in the channels with an isoscalar η -meson or Λ -hyperon, the total isospin I is unique and does not need to be specified.

3.2 Next-to-leading order amplitudes

At next-to-leading order $\mathcal{O}(q^2)$ one has the contributions from the diagrams in the second row of Fig. 1 (including crossed diagrams) involving the vertices from the Lagrangians $\mathcal{L}_{\phi B}^{(2,1/M_0)}$ and $\mathcal{L}_{\phi B}^{(2,\text{ct})}$. First, for the vertices from $\mathcal{L}_{\phi B}^{(2,1/M_0)}$, the amplitudes have the generic polynomial form,

$$V_{\pi,K,\eta}^{(1/M_0)}[a, b, c, d] = a \frac{1}{M_0 w_{\pi,K,\eta}^2 f_{\pi,K,\eta}^2} (bq^4 + cq^2 w_{\pi,K,\eta}^2 + dw_{\pi,K,\eta}^4), \quad (36)$$

$$W_{\pi,K,\eta}^{(1/M_0)}[e, f, g] = e \frac{1}{M_0 w_{\pi,K,\eta}^2 f_{\pi,K,\eta}^2} (fq^2 + gw_{\pi,K,\eta}^2). \quad (37)$$

We specify only the coefficients a, b, c, d for V and e, f, g for W by listing them in square brackets

$$T_{\pi N}^{(3/2)} = \left\{ V_{\pi}^{(1/M_0)} \left[\frac{(D+F)^2}{4}, -2z(1+z), \frac{-1-z}{(D+F)^2} + 2(2+z), -1 \right], \right. \\ \left. W_{\pi}^{(1/M_0)} \left[\frac{(D+F)^2}{2}, (1+z), -1 \right] \right\}, \quad (38)$$

$$T_{\pi N}^{(1/2)} = \left\{ V_{\pi}^{(1/M_0)} \left[\frac{(D+F)^2}{4}, z(1+z), \frac{2(1+z)}{(D+F)^2} - 2(1+2z), -1 \right], \right. \\ \left. W_{\pi}^{(1/M_0)} \left[\frac{(D+F)^2}{4}, -1-z, -2 \right] \right\}, \quad (39)$$

$$T_{\pi\Sigma}^{(2)} = \left\{ V_{\pi}^{(1/M_0)} \left[\frac{D^2 + 3F^2}{6}, -2z(1+z), \frac{-3(1+z)}{D^2 + 3F^2} + 2(2+z), -1 \right], \right. \\ \left. W_{\pi}^{(1/M_0)} \left[\frac{D^2 + 3F^2}{6}, 2(1+z), -2 \right] \right\}, \quad (40)$$

$$T_{\pi\Sigma}^{(1)} = \left\{ V_{\pi}^{(1/M_0)} \left[\frac{D^2 + 3F^2}{6}, 2z(1+z), \frac{3(1+z)}{D^2 + 3F^2} - 2(2+z), \frac{D^2 - 9F^2}{D^2 + 3F^2} \right], \right. \\ \left. W_{\pi}^{(1/M_0)} \left[\frac{D^2 + 3F^2}{3}, -(1+z), 1 \right] \right\}, \quad (41)$$

$$T_{\pi\Sigma}^{(0)} = \left\{ V_{\pi}^{(1/M_0)} \left[\frac{D^2 + 3F^2}{3}, -z(1+z), \frac{3(1+z)}{D^2 + 3F^2} - 2(z-1), \frac{-2D^2 + 3F^2}{D^2 + 3F^2} \right], \right. \\ \left. W_{\pi}^{(1/M_0)} \left[\frac{D^2 + 3F^2}{3}, 1+z, -4 \right] \right\}, \quad (42)$$

$$T_{\pi\Sigma}^{(3/2)} = \left\{ V_{\pi}^{(1/M_0)} \left[\frac{(D-F)^2}{4}, -2z(1+z), \frac{-(1+z)}{(D-F)^2} + 2(2+z), -1 \right], \right. \\ \left. W_{\pi}^{(1/M_0)} \left[\frac{(D-F)^2}{4}, 2(1+z), -2 \right] \right\}, \quad (43)$$

$$T_{\pi\Sigma}^{(1/2)} = \left\{ V_{\pi}^{(1/M_0)} \left[\frac{(D-F)^2}{4}, z(1+z), \frac{2(1+z)}{(D-F)^2} - 2(1+2z), -1 \right], \right. \\ \left. W_{\pi}^{(1/M_0)} \left[\frac{(D-F)^2}{4}, -1-z, -2 \right] \right\}, \quad (44)$$

$$T_{\pi\Lambda} = \left\{ -\frac{D^2 w_{\pi}^2}{3M_0 f_{\pi}^2}, 0 \right\}, \quad (45)$$

$$T_{KN}^{(1)} = \left\{ V_K^{(1/M_0)} \left[\frac{D^2 + 3F^2}{6}, -2z(1+z), \frac{-3(1+z)}{D^2 + 3F^2} + 2(2+z), -1 \right], \right. \\ \left. W_K^{(1/M_0)} \left[\frac{D^2 + 3F^2}{6}, 2(1+z), -2 \right] \right\}, \quad (46)$$

$$T_{KN}^{(0)} = \left\{ V_K^{(1/M_0)} \left[\frac{D(D-3F)}{3}, -2z(1+z), 2(2+z), -1 \right], \right. \\ \left. W_K^{(1/M_0)} \left[\frac{D(D-3F)}{3}, 2(1+z), -2 \right] \right\}, \quad (47)$$

$$T_{KN}^{(1)} = \left\{ V_K^{(1/M_0)} \left[\frac{(D-F)^2}{4}, 0, \frac{1+z}{(D-F)^2} - 2z, -1 \right], W_K^{(1/M_0)} \left[\frac{(D-F)^2}{2}, 0, -1 \right] \right\}, \quad (48)$$

$$T_{KN}^{(0)} = \left\{ V_K^{(1/M_0)} \left[\frac{(D+3F)^2}{12}, 0, \frac{9(1+z)}{(D+3F)^2} - 2z, -1 \right], W_K^{(1/M_0)} \left[\frac{(D+3F)^2}{6}, 0, -1 \right] \right\}, \quad (49)$$

$$T_{K\Sigma}^{(3/2)} = \left\{ V_K^{(1/M_0)} \left[\frac{(D+F)^2}{4}, -2z(1+z), \frac{-1-z}{(D+F)^2} + 2(z+2), -1 \right], \right. \\ \left. W_K^{(1/M_0)} \left[\frac{(D+F)^2}{4}, 2(1+z), -2 \right] \right\}, \quad (50)$$

$$T_{K\Sigma}^{(1/2)} = \left\{ V_K^{(1/M_0)} \left[\frac{(D+F)^2}{4}, z(1+z), \frac{2-2z+4z(D^2-DF+F^2)}{(D+F)^2} - 2, -\frac{D^2-4DF+F^2}{(D+F)^2} \right], \right. \\ \left. W_K^{(1/M_0)} \left[\frac{(D+F)^2}{4}, -1-z, -\frac{2(D^2-4DF+F^2)}{(D+F)^2} \right] \right\}, \quad (51)$$

$$T_{\overline{K}\Sigma}^{(3/2)} = \left\{ V_K^{(1/M_0)} \left[\frac{(D-F)^2}{4}, -2z(1+z), \frac{-1-z}{(D-F)^2} + 2(z+2), -1 \right], \right. \\ \left. W_K^{(1/M_0)} \left[\frac{(D-F)^2}{4}, 2(1+z), -2 \right] \right\}, \quad (52)$$

$$T_{\overline{K}\Sigma}^{(1/2)} = \left\{ V_K^{(1/M_0)} \left[\frac{(D-F)^2}{4}, z(1+z), \frac{2+2z-4z(D^2+DF+F^2)}{(D-F)^2} - 2, -\frac{D^2+4DF+F^2}{(D-F)^2} \right], \right. \\ \left. W_K^{(1/M_0)} \left[\frac{(D-F)^2}{4}, -1-z, -\frac{2(D^2+DF+F^2)}{(D-F)^2} \right] \right\}, \quad (53)$$

$$T_{K\Xi}^{(1)} = \left\{ V_K^{(1/M_0)} \left[\frac{(D+F)^2}{4}, 0, \frac{1+z}{(D+F)^2} - 2z, -1 \right], W_K^{(1/M_0)} \left[\frac{(D+F)^2}{2}, 0, -1 \right] \right\}, \quad (54)$$

$$T_{K\Xi}^{(0)} = \left\{ V_K^{(1/M_0)} \left[\frac{(D-3F)^2}{12}, 0, \frac{9(1+z)}{(D-3F)^2} - 2z, -1 \right], W_K^{(1/M_0)} \left[\frac{(D-3F)^2}{6}, 0, -1 \right] \right\}, \quad (55)$$

$$T_{\overline{K}\Xi}^{(1)} = \left\{ V_K^{(1/M_0)} \left[\frac{D^2+3F^2}{6}, -2z(1+z), -\frac{3(1+z)}{D^2+3F^2} + 4 + 2z, -1 \right], \right. \\ \left. W_K^{(1/M_0)} \left[\frac{D^2+3F^2}{6}, 2(1+z), -2 \right] \right\}, \quad (56)$$

$$T_{\overline{K}\Xi}^{(0)} = \left\{ V_K^{(1/M_0)} \left[\frac{D(D+3F)}{3}, -2z(1+z), 2(2+z), -1 \right], \right. \\ \left. W_K^{(1/M_0)} \left[\frac{D(D+3F)}{3}, 2(1+z), -2 \right] \right\}, \quad (57)$$

$$T_{K\Lambda} = \left\{ V_K^{(1/M_0)} \left[-\frac{1}{12}, z(1+z)(D-3F)^2, -2D^2 - 18F^2 + 12(1+z)DF, D^2 + 9F^2 \right], \right. \\ \left. W_K^{(1/M_0)} \left[\frac{1}{12}, (1+z)(D-3F)^2, -2(D^2 + 9F^2) \right] \right\}, \quad (58)$$

$$T_{\overline{K}\Lambda} = \left\{ V_K^{(1/M_0)} \left[-\frac{1}{12}, z(1+z)(D+3F)^2, -2D^2 - 18F^2 - 12(1+z)DF, D^2 + 9F^2 \right], \right. \\ \left. W_K^{(1/M_0)} \left[\frac{1}{12}, (1+z)(D+3F)^2, -2(D^2 + 9F^2) \right] \right\}, \quad (59)$$

$$T_{\eta N} = \left\{ V_\eta^{(1/M_0)} \left[\frac{(D-3F)^2}{12}, (-1-z)z, 2+z, -1 \right], W_\eta^{(1/M_0)} \left[\frac{(D-3F)^2}{12}, 1+z, -1 \right] \right\}, \quad (60)$$

$$T_{\eta\Sigma} = \left\{ -\frac{D^2 w_\eta^2}{3f_\eta^2 M_0}, 0 \right\}, \quad (61)$$

$$T_{\eta\Xi} = \left\{ V_\eta^{(1/M_0)} \left[\frac{(D+3F)^2}{12}, (-1-z)z, 2+z, -1 \right], W_\eta^{(1/M_0)} \left[\frac{(D+3F)^2}{12}, 1+z, -1 \right] \right\}, \quad (62)$$

$$T_{\eta\Lambda} = \left\{ -\frac{D^2 w_\eta^2}{3f_\eta^2 M_0}, 0 \right\}. \quad (63)$$

For the explicit chiral symmetry breaking part of $\mathcal{L}_{\phi B}^{(2,ct)}$, we introduce the combinations of LECs and meson masses

$$\begin{aligned} \alpha_N &= 3(b_0 + b_D - b_F)m_\eta^2 + (3b_0 + b_D + 3b_F)m_\pi^2, \\ \alpha_\Sigma &= 4b_D m_\pi^2 + 3b_0(m_\pi^2 + m_\eta^2), \\ \alpha_\Xi &= 3(b_0 + b_D + b_F)m_\eta^2 + (3b_0 + b_D - 3b_F)m_\pi^2, \\ \alpha_\Lambda &= 4b_D m_\pi^2 + 3b_0(m_\pi^2 + m_\eta^2) \end{aligned} \quad (64)$$

in order to make the following expressions for the amplitudes $\{V_{MB}^{(I)}, W_{MB}^{(I)}\}$ more compact. In this pair notation the amplitudes read

$$\begin{aligned} T_{\pi N}^{(3/2)} &= \left\{ \frac{1}{2f_\pi^2 w_\pi^2} [\alpha_N z(D+F)^2 q^2 - 4(2b_0 + b_D + b_F)m_\pi^2 w_\pi^2 - 4C_1 z q^2 w_\pi^2 + 4(C_1 + C_2)w_\pi^4], \right. \\ &\quad \left. - \frac{1}{2f_\pi^2 w_\pi^2} [\alpha_N(D+F)^2 + 4C_3 w_\pi^2] \right\}, \end{aligned} \quad (65)$$

$$\begin{aligned} T_{\pi N}^{(1/2)} &= \left\{ \frac{1}{2f_\pi^2 w_\pi^2} [\alpha_N z(D+F)^2 q^2 - 4(2b_0 + b_D + b_F)m_\pi^2 w_\pi^2 - 4C_1 z q^2 w_\pi^2 + 4(C_1 + C_2)w_\pi^4], \right. \\ &\quad \left. \frac{1}{f_\pi^2 w_\pi^2} [\alpha_N(D+F)^2 + 4C_3 w_\pi^2] \right\}, \end{aligned} \quad (66)$$

$$\begin{aligned} T_{KN}^{(1)} &= \left\{ \frac{1}{12f_K^2 w_K^2} [3\alpha_\Sigma(D-F)^2 q^2 z + \alpha_\Lambda(D+3F)^2 q^2 z - 48(b_0 + b_D)m_K^2 w_K^2 - 24C_4 z q^2 w_K^2 \right. \\ &\quad \left. + 24(C_4 + C_5)w_K^4], -\frac{1}{12f_K^2 w_K^2} [3\alpha_\Sigma(D-F)^2 + \alpha_\Lambda(D+3F)^2 + 12C_6 w_K^2] \right\}, \end{aligned} \quad (67)$$

$$\begin{aligned} T_{KN}^{(0)} &= \left\{ \frac{1}{12f_K^2 w_K^2} [9\alpha_\Sigma(D-F)^2 q^2 z - \alpha_\Lambda(D+3F)^2 q^2 z - 48(b_0 - b_F)m_K^2 w_K^2 + 24C_7 z q^2 w_K^2 \right. \\ &\quad \left. - 24(C_7 + C_8)w_K^4], \frac{1}{12f_K^2 w_K^2} [-9\alpha_\Sigma(D-F)^2 + \alpha_\Lambda(D+3F)^2 + 12C_9 w_K^2] \right\}, \end{aligned} \quad (68)$$

$$\begin{aligned} T_{KN}^{(1)} &= \left\{ \frac{1}{2f_K^2 w_K^2} [\alpha_\Sigma(D-F)^2 q^2 z - 4(2b_0 + b_D - b_F)m_K^2 w_K^2 - 2(C_4 - C_7)z q^2 w_K^2 \right. \\ &\quad \left. + 2(C_4 + C_5 - C_7 - C_8)w_K^4], \frac{1}{2f_K^2 w_K^2} [\alpha_\Sigma(D-F)^2 + (C_6 - C_9)w_K^2] \right\}, \end{aligned} \quad (69)$$

$$T_{KN}^{(0)} = \left\{ \frac{1}{6f_K^2 w_K^2} [\alpha_\Lambda (D + 3F)^2 q^2 z - 12(2b_0 + 3b_D + b_F) m_K^2 w_K^2 - 6(3C_4 + C_7) z q^2 w_K^2 + 6(3C_4 + C_7 + 3C_5 + C_8) w_K^4], \frac{1}{6f_K^2 w_K^2} [\alpha_\Lambda (D + 3F)^2 + 3(3C_6 + C_9) w_K^2] \right\}, \quad (70)$$

$$T_{\pi\Sigma}^{(2)} = \left\{ \frac{1}{3f_\pi^2 w_\pi^2} [(\alpha_\Lambda D^2 + 3\alpha_\Sigma F^2) q^2 z - 12(b_0 + b_D) m_\pi^2 w_\pi^2 - 6C_4 z q^2 w_\pi^2 + 6(C_4 + C_5) w_\pi^4], -\frac{1}{3f_\pi^2 w_\pi^2} [\alpha_\Lambda D^2 + 3\alpha_\Sigma F^2 + 3C_6 w_\pi^2] \right\}, \quad (71)$$

$$T_{\pi\Sigma}^{(1)} = \left\{ -\frac{1}{3f_\pi^2 w_\pi^2} [(\alpha_\Lambda D^2 + 3\alpha_\Sigma F^2) q^2 z + 12(b_0 + b_D) m_\pi^2 w_\pi^2 + 6(C_4 - 2b_4) z q^2 w_\pi^2 - 6(C_4 - 2b_4 + C_5 - 2b_8) w_\pi^4], \frac{1}{3f_\pi^2 w_\pi^2} [\alpha_\Lambda D^2 + 3\alpha_\Sigma F^2 + 3C_6 w_\pi^2] \right\}, \quad (72)$$

$$T_{\pi\Sigma}^{(0)} = \left\{ \frac{4}{3f_\pi^2 w_\pi^2} [(\alpha_\Lambda D^2 + 3\alpha_\Sigma F^2) q^2 z - 3(b_0 + b_D) m_\pi^2 w_\pi^2 - \frac{3}{2}(C_4 + 3b_4) z q^2 w_\pi^2 + \frac{1}{2}(C_4 + 3b_4 + C_5 + 3b_8) w_\pi^4], \frac{2}{3f_\pi^2 w_\pi^2} [\alpha_\Lambda D^2 + 3\alpha_\Sigma F^2 + 3C_6 w_\pi^2] \right\}, \quad (73)$$

$$T_{\pi\Xi}^{(3/2)} = \left\{ \frac{1}{2f_\pi^2 w_\pi^2} [\alpha_\Xi (D - F)^2 q^2 z - 4(2b_0 + b_D - b_F) m_\pi^2 w_\pi^2 - 2(C_4 - C_7) z q^2 w_\pi^2 + 2(C_4 - C_7 + C_5 - C_8) w_\pi^4], -\frac{1}{2f_\pi^2 w_\pi^2} [\alpha_\Xi (D - F)^2 + (C_6 - C_9) w_\pi^2] \right\}, \quad (74)$$

$$T_{\pi\Xi}^{(1/2)} = \left\{ \frac{1}{2f_\pi^2 w_\pi^2} [\alpha_\Xi (D - F)^2 q^2 z - 4(2b_0 + b_D - b_F) m_\pi^2 w_\pi^2 - 2(C_4 - C_7) z q^2 w_\pi^2 + 2(C_4 - C_7 + C_5 - C_8) w_\pi^4], \frac{1}{f_\pi^2 w_\pi^2} [\alpha_\Xi (D - F)^2 + (C_6 - C_9) w_\pi^2] \right\}, \quad (75)$$

$$T_{\pi\Lambda} = \left\{ \frac{2}{3f_\pi^2} [-2(3b_0 + b_D) m_\pi^2 - (2C_1 - C_7 + b_4) z q^2 + (2C_1 - C_7 + b_4 + 2C_2 - C_8 + b_8) w_\pi^2], 0 \right\}, \quad (76)$$

$$T_{K\Sigma}^{(3/2)} = \left\{ \frac{1}{2f_K^2 w_K^2} [\alpha_\Xi (D + F)^2 q^2 z - 4(2b_0 + b_D + b_F) m_K^2 w_K^2 - 4C_1 z q^2 w_K^2 + 4(C_1 + C_2) w_K^4], -\frac{1}{2f_K^2 w_K^2} [\alpha_\Xi (D + F)^2 + 4C_3 w_K^2] \right\}, \quad (77)$$

$$T_{K\Sigma}^{(1/2)} = \left\{ \frac{1}{4f_K^2 w_K^2} [3\alpha_N (D - F)^2 q^2 z - \alpha_\Xi (D + F)^2 q^2 z - 8(2b_0 + b_D - 2b_F) m_K^2 w_K^2 + 2(2C_1 - 3C_4 + 3C_7) z q^2 w_K^2 - 2(2C_1 - 3C_4 + 3C_7 + 2C_2 - 3C_5 + 3C_8) w_K^4], \frac{1}{4f_K^2 w_K^2} [3\alpha_N (D - F)^2 + \alpha_\Xi (D + F)^2 + (4C_3 + 3C_6 - 3C_9) w_K^2] \right\}, \quad (78)$$

$$T_{K\Sigma}^{(3/2)} = \left\{ \frac{1}{2f_K^2 w_K^2} [\alpha_N (D-F)^2 q^2 z - 4(2b_0 + b_D - b_F) m_K^2 w_K^2 - 2(C_4 - C_7) z q^2 w_K^2 + 2(C_4 - C_7 + C_5 - C_8) w_K^4], -\frac{1}{2f_K^2 w_K^2} [\alpha_N (D-F)^2 + (C_6 - C_9) w_K^2] \right\}, \quad (79)$$

$$T_{K\Sigma}^{(1/2)} = \left\{ \frac{1}{4f_K^2 w_K^2} [-\alpha_N (D-F)^2 q^2 z + 3\alpha_\Xi (D+F)^2 q^2 z - 8(2b_0 + b_D + 2b_F) m_K^2 w_K^2 - 2(6C_1 - C_4 + C_7) z q^2 w_K^2 + 2(6C_1 - C_4 + C_7 + 6C_2 - C_5 + C_8) w_K^4], \frac{1}{4f_K^2 w_K^2} [\alpha_N (D-F)^2 + 3\alpha_\Xi (D+F)^2 + (12C_3 + C_6 - C_9) w_K^2] \right\}, \quad (80)$$

$$T_{K\Xi}^{(1)} = \left\{ \frac{1}{2f_K^2 w_K^2} [\alpha_\Sigma (D+F)^2 q^2 z - 4(2b_0 + b_D + b_F) m_K^2 w_K^2 - 4C_1 z q^2 w_K^2 + 4(C_1 + C_2) w_K^4], \frac{1}{2f_K^2 w_K^2} [\alpha_\Sigma (D+F)^2 + 4C_3 w_K^2] \right\}, \quad (81)$$

$$T_{K\Xi}^{(0)} = \left\{ \frac{1}{6f_K^2 w_K^2} [\alpha_\Lambda (D-3F)^2 q^2 z + 12(-2b_0 - 3b_D + b_F) m_K^2 w_K^2 + 12(C_1 - 2C_4) z q^2 w_K^2 - 12(C_1 - 2C_4 + C_2 - 2C_5) w_K^4], \frac{1}{6f_K^2 w_K^2} [\alpha_\Lambda (D-3F)^2 + 12(-C_3 + C_6) w_K^2] \right\}, \quad (82)$$

$$T_{K\Xi}^{(1)} = \left\{ \frac{1}{12f_K^2 w_K^2} [\alpha_\Lambda (D-3F)^2 q^2 z + 3\alpha_\Sigma (D+F)^2 q^2 z - 48(b_0 + b_D) m_K^2 w_K^2 - 24C_4 z q^2 w_K^2 + 24(C_4 + C_5) w_K^4], -\frac{1}{12f_K^2 w_K^2} [\alpha_\Lambda (D-3F)^2 + 3\alpha_\Sigma (D+F)^2 + 12C_6 w_K^2] \right\}, \quad (83)$$

$$T_{K\Xi}^{(0)} = \left\{ -\frac{1}{12f_K^2 w_K^2} [\alpha_\Lambda (D-3F)^2 q^2 z - 9\alpha_\Sigma (D+F)^2 q^2 z + 48(b_0 + b_F) m_K^2 w_K^2 + 24(2C_1 - C_4) z q^2 w_K^2 - 24(2C_1 - C_4 + 2C_2 - C_5) w_K^4], \frac{1}{12f_K^2 w_K^2} [\alpha_\Lambda (D-3F)^2 - 9\alpha_\Sigma (D+F)^2 - 12(4C_3 - C_6) w_K^2] \right\}, \quad (84)$$

$$T_{K\Lambda} = \left\{ \frac{1}{12f_K^2 w_K^2} [\alpha_\Xi (D-3F)^2 q^2 z + \alpha_N (D+3F)^2 q^2 z - 8(6b_0 + 5b_D) m_K^2 w_K^2 - 2(-8b_4 + 2C_1 + 9C_4 - C_7) z q^2 w_K^2 + 2(-8b_4 + 2C_1 + 9C_4 - C_7 - 8b_8 + 2C_2 + 9C_5 - C_8) w_K^4], \frac{1}{12f_K^2 w_K^2} [-\alpha_\Xi (D-3F)^2 + \alpha_N (D+3F)^2 + 3(4C_3 - C_6 + C_9) w_K^2] \right\}, \quad (85)$$

$$T_{K\Lambda} = \left\{ \frac{1}{12f_K^2 w_K^2} [\alpha_\Xi (D-3F)^2 q^2 z + \alpha_N (D+3F)^2 q^2 z - 8(6b_0 + 5b_D) m_K^2 w_K^2 - 2(-8b_4 + 2C_1 + 9C_4 - C_7) z q^2 w_K^2 + 2(-8b_4 + 2C_1 + 9C_4 - C_7 - 8b_8 + 2C_2 + 9C_5 - C_8) w_K^4], \frac{1}{12f_K^2 w_K^2} [\alpha_\Xi (D-3F)^2 - \alpha_N (D+3F)^2 - 3(4C_3 - C_6 + C_9) w_K^2] \right\}, \quad (86)$$

$$T_{\eta N} = \left\{ \frac{1}{6f_\eta^2 w_\eta^2} [\alpha_N (D - 3F)^2 q^2 z - 32(b_0 + b_D - b_F) m_K^2 w_\eta^2 + 4(2b_0 + 3b_D - 5b_F) m_\pi^2 w_\eta^2 + 4(2b_4 + C_1 - 3C_4 + C_7) z q^2 w_\eta^2 - 4(2b_4 + C_1 - 3C_4 + C_7 + 2b_8 + C_2 - 3C_5 + C_8) w_\eta^4], 0 \right\}, \quad (87)$$

$$T_{\eta \Sigma} = \left\{ \frac{2}{3f_\eta^2} [-8b_0 m_K^2 + 2(b_0 - b_D) m_\pi^2 - (b_4 + 2C_1 - C_7) z q^2 + (b_4 + 2C_1 - C_7 + b_8 + 2C_2 - C_8) w_\eta^2], 0 \right\}, \quad (88)$$

$$T_{\eta \Xi} = \left\{ \frac{1}{6f_\eta^2 w_\eta^2} [\alpha_\Xi (D + 3F)^2 q^2 z - 32(b_0 + b_D + b_F) m_K^2 w_\eta^2 + 4(2b_0 + 3b_D + 5b_F) m_\pi^2 w_\eta^2 - 2(-4b_4 + 4C_1 + 3C_4 + C_7) z q^2 w_\eta^2 + 2(-4b_4 + 4C_1 + 3C_4 + C_7 - 4b_8 + 4C_2 + 3C_5 + C_8) w_\eta^4], 0 \right\}, \quad (89)$$

$$T_{\eta \Lambda} = \left\{ \frac{2}{9f_\eta^2} [-8(3b_0 + 4b_D) m_K^2 + 2(3b_0 + 7b_D) m_\pi^2 - 9(b_4 + C_4) z q^2 + 9(b_4 + C_4 + b_8 + C_5) w_\eta^2], 0 \right\}. \quad (90)$$

Here we have introduced the nine linear combinations

$$\begin{aligned} C_1 &= b_1 + b_2 + 2b_3, & C_2 &= b_5 + b_6 + 2b_7, & C_3 &= b_9 + b_{10}, \\ C_4 &= 2b_1 + 2b_3 + b_4, & C_5 &= 2b_5 + 2b_7 + b_8, & C_6 &= 4b_{10} + b_{11}, \\ C_7 &= 2b_2 - 2b_3 + b_4, & C_8 &= 2b_6 - 2b_7 + b_8, & C_9 &= 4b_9 + b_{11}, \end{aligned} \quad (91)$$

of the low-energy constants $b_i (i = 1, \dots, 11)$ in order to get a more compact representation.

3.3 Next-to-next-to-leading order amplitudes

At the third order $\mathcal{O}(q^3)$ one has contributions from one-loop diagrams and counterterms. The nonvanishing one-loop diagrams generated by the vertices of $\mathcal{L}_{\phi\phi}^{(2)}$ and $\mathcal{L}_{\phi B}^{(1)}$ are shown in Fig. 2. The counterterm contributions estimated from resonance exchange were found to be much smaller than the chiral loop contributions [14, 15, 16, 23, 24]. Therefore, we are not considering the counterterms contributions when calculating T-matrices at $\mathcal{O}(q^3)$ in this paper. The one-loop amplitudes are tedious to evaluate, and we give only occurring loop functions in Appendix A. We use dimensional regularization and minimal subtraction to evaluate divergent loop integrals [25, 26, 27, 28, 29]. We use $f_{\pi, K, \eta}$ for pion, kaon, eta-baryon scattering amplitudes from loops instead of the value f in the chiral limit. The differences appear at higher order.

4 Calculating phase shifts and scattering lengths

The partial wave amplitudes $f_j^{(I)}(q)$, where $j = l \pm 1/2$ refers to the total angular momentum and l to orbital angular momentum, are obtained from the non spin-flip and spin-flip amplitudes by a projection:

$$f_{l\pm 1/2}^{(I)}(q) = \frac{M_B}{8\pi(w_M + E_B)} \int_{-1}^{+1} dz \left\{ V_{MB}^{(I)}(q) P_l(z) + q^2 W_{MB}^{(I)}(q) [P_{l\pm 1}(z) - z P_l(z)] \right\}, \quad (92)$$

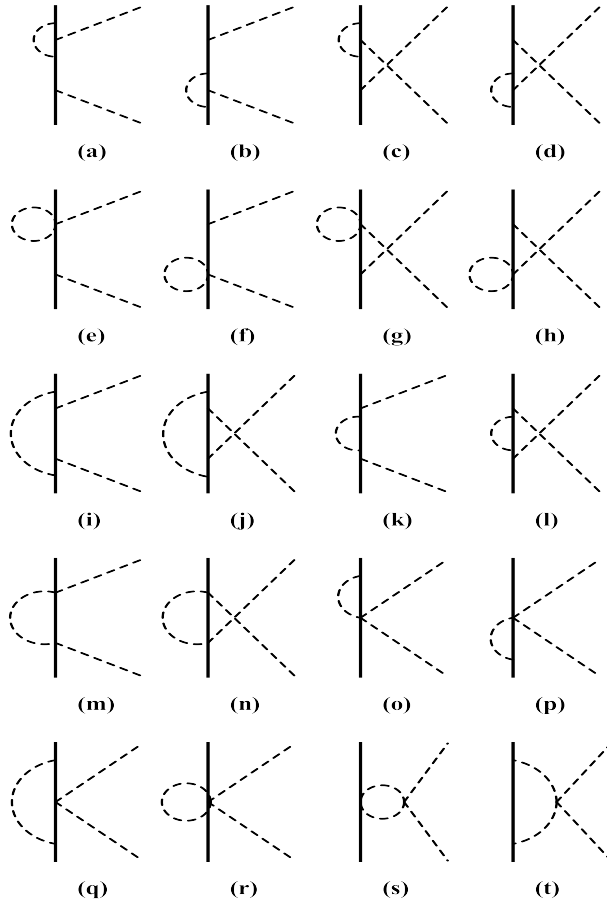


Figure 2: Nonvanishing one-loop diagrams contributing at third chiral order. Diagrams with self-energy correction on external meson or baryon lines are not shown.

where $P_l(z)$ denotes the conventional Legendre polynomial and $w_M + E_B = \sqrt{m_M^2 + q^2} + \sqrt{M_B^2 + q^2}$ is the total center-of-mass energy. For the energy range considered in this paper, the phase shifts $\delta_{l\pm 1/2}^{(I)}(q)$ are calculated by (also see Refs. [10, 30])

$$\delta_{l\pm 1/2}^{(I)}(q) = \arctan[q \operatorname{Re} f_{l\pm 1/2}^{(I)}(q)]. \quad (93)$$

Based upon relativistic kinematics, there is the relation between the center-of-mass momentum q and the momentum p_{lab} of the incident meson in the laboratory system,

$$q^2 = \frac{M_B^2 p_{\text{lab}}^2}{m_M^2 + M_B^2 + 2M_B \sqrt{m_M^2 + p_{\text{lab}}^2}}. \quad (94)$$

The scattering lengths for s-waves and the scattering volumes for p-waves are obtained by approaching the threshold [31]

$$a_{l\pm 1/2}^{(I)} = \lim_{q \rightarrow 0} q^{-2l} f_{l\pm 1/2}^{(I)}(q). \quad (95)$$

5 Results and discussion

Before making predictions, we have to determine the low-energy constants. The parameters M_0, b_D, b_F and b_0 have been determined in our previous paper [19]. After the regrouping in Eq. (91), we need to determine the 9 combinations $C_{1,\dots,9}$. Throughout this paper, we also use $m_\pi = 139.57$ MeV, $m_K = 493.68$ MeV, $m_\eta = 547.86$ MeV, $M_N = 938.9$ MeV, $M_\Sigma = 1193.4$ MeV, $M_\Xi = 1318.3$ MeV, $M_\Lambda = 1115.7$ MeV, $f_\pi = 92.2$ MeV, $f_K = 111$ MeV, and $f_\eta = 1.2f_\pi$ [32]. For the axial vector coupling constants we take the values $D = 0.8$ and $F = 0.5$. We also set the scale λ equal to the chiral symmetry breaking scale, $\lambda = 4\pi f_\pi = 1.16$ GeV.

We determine the 9 LEC combinations $C_{1,\dots,9}$ by using the phase shifts of the WI08 solution and the SP92 solution for πN and KN scattering analysis [33, 34, 35], respectively. Since both solutions include no uncertainties for the phase shifts, we choose a common uncertainty of $\pm 4\%$ to all phase shifts before the fitting procedure. Actually, this uncertainty is arbitrary and it does not change the results for the phase shifts but only the respective $\chi^2/\text{d.o.f}$. For fitting the parameters $C_{1,2,3}$, we use the data in the $S31$, $P31$, and $P33$ partial waves for πN scattering between 50 and 90 MeV pion lab-momentum. We obtain

$$C_1 = -7.76 \pm 0.19 \text{ GeV}^{-1}, \quad C_2 = 6.52 \pm 0.19 \text{ GeV}^{-1}, \quad C_3 = 3.22 \pm 0.10 \text{ GeV}^{-1}, \quad (96)$$

with a $\chi^2/\text{d.o.f} \simeq 1.2$. For fitting $C_{4,5,6}$ we use the data in the $S11$, $P11$ and $P13$ partial waves of KN scattering between 50 and 90 MeV kaon lab-momentum. For determining $C_{7,8,9}$, we fit to the data of the $S01$, $P01$, and $P03$ partial waves at $p_K = (110, 120, 130, 140, 150)$ MeV. The resulting LECs have the values

$$C_4 = -0.99 \pm 0.05 \text{ GeV}^{-1}, \quad C_5 = 0.22 \pm 0.06 \text{ GeV}^{-1}, \quad C_6 = 6.36 \pm 0.09 \text{ GeV}^{-1}, \quad (97)$$

with a $\chi^2/\text{d.o.f} \simeq 0.9$ and

$$C_7 = -1.45 \pm 0.09 \text{ GeV}^{-1}, \quad C_8 = 2.48 \pm 0.09 \text{ GeV}^{-1}, \quad C_9 = 5.06 \pm 0.11 \text{ GeV}^{-1}, \quad (98)$$

with a $\chi^2/\text{d.o.f} \simeq 2.0$. The uncertainty for the respective parameters is purely statistical and it measures how much a particular parameter can be changed while maintaining a good description of the fitted data, as detailed in Refs. [36, 37]. The corresponding S - and P -waves phase shifts are shown in Fig. 3. Note that the partial waves are denoted by $L_{2I,2J}$ with L the angular momentum, I the total isospin, and J the total angular momentum. If I is fixed, we use the simpler notation L_{2J} . When fitting $C_{7,8,9}$, the $\chi^2/\text{d.o.f}$ is larger than 1 because of the small uncertainties of the phase shifts in the $S01$, $P01$, and $P03$ partial waves. If we assign an uncertainties of $\pm 5\%$ to these phase shifts, the $\chi^2/\text{d.o.f}$ reduces to 1.3 while the parameters $C_{7,8,9}$ remain unchanged. This means that the uncertainty of the KN scattering data is larger than those of πN scattering. Our fitting procedure is therefore reasonable. For the partial waves in Fig. 3, the description of the phase shifts is in agreement with the empirical phase shifts below 150 MeV. However, there exists a zero in the $P31$ wave of πN scattering, which is not in agreement with the empirical phase shifts. Furthermore, the $P33$ wave of πN scattering is also underestimated due to the presence of the prominent $\Delta(1232)$ resonance.

Now we have fixed the nine constants $C_{1,\dots,9}$. But there are still two more parameters, namely b_4 and b_8 . We have no further data available to fix these two parameters. Therefore, we use the values determined from elastic and inelastic scatterings [38]. Comparing our heavy-baryon Lagrangian $\mathcal{L}_{\phi B}^{(2,\text{ct})}$ with the corresponding Lagrangian of Refs. [38, 39], one obtains the relations $2(b_4 + b_8) = d_1$ and $-2b_4 = g_1$. This give us the estimates $b_4 = -0.73 \text{ GeV}^{-1}$ and $b_8 = 0.81 \text{ GeV}^{-1}$.

In order to check the consistency of the ChPT framework for different observables, we determine some combinations of the low-energy constants from scattering lengths. We evaluate the threshold T-matrices at $q = 0$ to obtain the scattering lengths. We use the three scattering lengths $a_{\pi N}^{(3/2)} = -0.11 \text{ fm}$ from the WI08 solution [33, 35], $a_{KN}^{(1)} = -0.33 \text{ fm}$ and $a_{KN}^{(0)} = 0.00 \text{ fm}$ from the SP92 solution [34] and determine the three LEC combinations as

$$C_1 + C_2 = -1.16 \text{ GeV}^{-1}, \quad C_4 + C_5 = -0.85 \text{ GeV}^{-1}, \quad C_7 + C_8 = 1.00 \text{ GeV}^{-1}. \quad (99)$$

The same combinations of low-energy constants determined from fitting to phase shifts are $C_1 + C_2 = -1.24 \text{ GeV}^{-1}$ (see Eq. (96)), $C_4 + C_5 = -0.77 \text{ GeV}^{-1}$ (see Eq. (97)) and $C_7 + C_8 = 1.03 \text{ GeV}^{-1}$ (see Eq. (98)). These results are within errors consistent with the LEC combinations in Eq. (99).

Next, we can predict phase shifts for octet-meson-baryon scattering. Let us look at the $S11$ -, $P11$ - and $P13$ -waves of πN scattering. We can compare our results with the phase shifts of the WI08 solution shown in Fig. 4. In the $S11$ - and $P13$ -waves, the phase shifts are overestimated at large pion momenta, but agree with the empirical phase shifts blow 50 MeV. For the $P11$ -wave the prediction is not good. The reason is the presence of the Roper resonance. We obtain only a downward bending towards attraction at 250 MeV in $P11$ -wave.

We can also predict phase shifts for the other scattering channels which are shown in Figs. 5–8. There exists bending in $P41$ -, $P43$ -, and $P23$ -wave of $\pi\Sigma$ scattering. Considering our prediction

for P_{11} -wave of πN scattering, there maybe exist resonances in the three waves. We obviously fail to generate the $\Lambda(1405)$ resonance. Nonperturbative methods [40, 41, 42, 43, 44] in S_{01} -wave of $\bar{K}N$ scattering are required to generate dynamically the $\Lambda(1405)$. Nevertheless we obtain a large attractive phase shift in this wave. Compared to the $S_{01}(\bar{K}N)$ wave, there exist similar features in $S_{01}(\pi\Sigma)$, $S_{01}(K\Xi)$ and $S_{11}(\bar{K}\Sigma)$ waves. It is possible to generate dynamically resonances in these waves through nonperturbative resummation techniques.

Then we calculate the scattering lengths through the use of Eq. (96) order by order. The results are shown in Tables 1–4. The scattering lengths are obtained by using an incident meson momentum $p_{\text{lab}} = 10$ MeV to approximate its value at threshold. There are not yet enough empirical data for comparison. Instead, we present the scattering lengths calculated through the threshold T-matrices by Liu and Zhu [15] in Tables 1–4. Our values are agreement with Liu’s results order by order. There is a slight difference to Liu’s results because different input data such as $\sigma_{\pi N}$ were used. Note that we only give the real parts of the scattering lengths in our paper. For the imaginary parts of the scattering lengths we obtain the almost same results as Ref. [15].

We can use the value of the nucleon σ -term $\sigma_{\pi N}$ to fix the M_0 , b_0 , b_D and b_F above. We failed to fix the four constants through fitting the phase shifts directly. But if we set a value of the baryon mass M_0 in the chiral limit, we can successfully predict the nucleon σ -term $\sigma_{\pi N}$ through fitting the data in the S_{31} , P_{31} , and P_{33} waves of πN scattering between 50 and 90 MeV to determine C_1 , C_2 , C_3 , α_N and $B_\pi = (b_D + b_F + 2b_0)m_\pi^2$ and using Eq. (6.13a) of Ref. [26],

$$\begin{aligned} \sigma_{\pi N} = & -\frac{m_\pi^2}{64\pi f_\pi^2} \left[9(D+F)^2 m_\pi + (5D^2 - 6DF + 9F^2)m_K + \frac{1}{3}(D-3F)^2 m_\eta \right] \\ & - 2(b_D + b_F + 2b_0)m_\pi^2. \end{aligned} \quad (100)$$

However, a different M_0 was obtained in other works [45, 46, 47, 48]. Then we present the relation between M_0 and $\sigma_{\pi N}$ in Fig. 9. For values of M_0 ranging from 500 MeV to 1000 MeV, we obtain a same $\chi^2/\text{d.o.f} \simeq 0.98$ (here, we set the uncertainties of $\pm 2\%$ to the phase shifts). That means the fitting is not sensitive to the value of the M_0 . We show the corresponding S - and P -waves phase shifts in Fig. 10 for $M_0 = 751$ MeV. The P_{33} wave of πN scattering is still underestimated because of the $\Delta(1232)$ resonance. The prediction for the P_{11} wave of πN scattering shows an interesting feature. The repulsion turns into the attraction at around 250 MeV, as the empirical phase shifts.

Let us look at the predictions for $\sigma_{\pi N}$ from different M_0 values, shown in Table 5. For $M_0 = 751$ MeV from lattice QCD [45], we obtain also $\sigma_{\pi N} = 58.7$ MeV in agreement with Ref. [49]. For $M_0=882$ MeV and 880 MeV, our predictions for $\sigma_{\pi N}$ are agreement with the results from Refs. [46, 48] within errors. To sum up, we obtain a reasonable relation between M_0 and $\sigma_{\pi N}$.

Finally, we discuss the convergence. For pion-baryon scattering; see Fig. 5, we find the phase shifts converge well in the following waves: $P_{31}(\pi N)$, $S_{11}(\pi N)$, $P_{43}(\pi\Sigma)$, $S_{21}(\pi\Sigma)$, $P_{23}(\pi\Sigma)$, $P_{01}(\pi\Sigma)$, $P_{03}(\pi\Sigma)$, $P_3(\pi\Lambda)$. There are about 33% waves that converge well. For kaon-baryon scattering; see Fig. 6, there are about 71% waves including $S_{21}(KN)$, $P_{21}(KN)$, $P_{23}(KN)$, $P_{01}(KN)$, $P_{03}(KN)$, $S_{31}(K\Sigma)$, $P_{31}(K\Sigma)$, $P_{33}(K\Sigma)$, $P_{11}(K\Sigma)$, $P_{13}(K\Sigma)$, $P_{21}(K\Xi)$, $P_{23}(K\Xi)$, $P_{03}(K\Xi)$, $S_1(K\Lambda)$ and $P_1(K\Lambda)$ to converge well. For antikaon-baryon scattering; see Fig. 7, there are about 71% waves including $S_{21}(\bar{K}N)$, $P_{21}(\bar{K}N)$, $P_{01}(\bar{K}N)$, $P_{03}(\bar{K}N)$, $P_{31}(\bar{K}\Sigma)$, $P_{11}(\bar{K}\Sigma)$, $P_{13}(\bar{K}\Sigma)$, $S_{21}(\bar{K}\Xi)$, $P_{21}(\bar{K}\Xi)$, $P_{23}(\bar{K}\Xi)$, $P_{01}(\bar{K}\Xi)$, $P_{03}(\bar{K}\Xi)$, $S_1(\bar{K}\Lambda)$, $P_1(\bar{K}\Lambda)$ and $P_3(\bar{K}\Lambda)$ to converge well. The convergence of the antikaon-baryon scattering is almost same than the kaon-baryon scattering. For eta-baryon scattering; see Fig. 8, there are about 83% waves except for $S_1(\eta N)$ and $P_1(\eta\Xi)$ to converge well. It seems that the larger the meson has a mass, the better the phase shift converge. That is unreasonable, and a higher-order $\mathcal{O}(q^4)$ calculation is needed. However, we find that the convergence of the P -wave is better than the S -wave.

In summary, we have calculated the T-matrices of meson-baryon scattering to one-loop order in SU(3) HB χ PT. We fitted to phase shifts of πN and KN scattering in order to determine the LECs. We predict the other channels by using these LECs and find there maybe exist resonances in the $P_{41}(\pi\Sigma)$, $P_{43}(\pi\Sigma)$, $P_{23}(\pi\Sigma)$, $S_{01}(\pi\Sigma)$, $S_{01}(K\Xi)$ and $S_{11}(\bar{K}\Sigma)$ waves. We also discuss the relation between the baryon mass M_0 in the chiral limit with the nucleon σ -term $\sigma_{\pi N}$, and obtain a reasonable result. Finally, we check the convergence of the meson-baryon scattering and find that our predictions for P -waves are better than S -waves. We expect to obtain improved results for meson-baryon scattering in future higher-order and nonperturbative calculations.

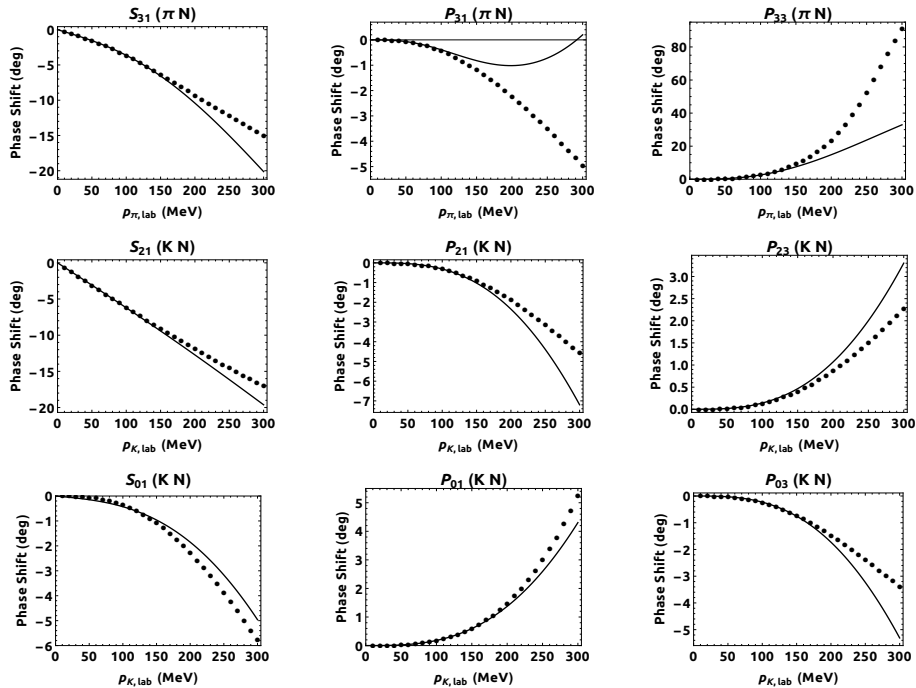


Figure 3: Fits and predictions for the WI08 and SP92 phase shifts in πN and $K N$ scatterings versus the pion and kaon laboratory momenta, respectively. Fitting in πN waves are the data between 50 and 90 MeV, while fitting $K N$ data at $p_{\text{lab}} = (110, 120, 130, 140, 150)$ MeV. For higher and lower energies, the phase shifts are predicted. The dotted lines denote the results from SAID [35] and the solid lines refer to our calculations.

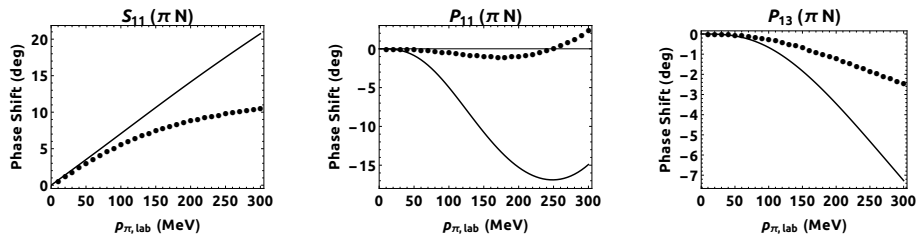


Figure 4: Predictions for the WI08 phase shifts in πN scatterings versus the pion laboratory momentum. The dotted lines denote the results from SAID [35] and the solid lines refer to our calculations.

Table 1: Values of the pion-baryon scattering lengths for our calculations in comparison to the results of Liu [15]. The scattering lengths are in units of fm.

Our Prediction	$\mathcal{O}(q)$	$\mathcal{O}(q^2)$	$\mathcal{O}(q^3)$	Total	Liu*	$\mathcal{O}(q)$	$\mathcal{O}(q^2)$	$\mathcal{O}(q^3)$	Total
$a_{\pi N}^{(3/2)}$	-0.11	0.06	-0.06	-0.12	-0.11	0.04	-0.06	-0.13	
$a_{\pi N}^{(1/2)}$	0.22	0.06	-0.00	0.28	0.22	0.04	-0.00	0.26	
$a_{\pi\Sigma}^{(2)}$	-0.23	0.06	-0.07	-0.24	-0.23	0.06	-0.07	-0.24	
$a_{\pi\Sigma}^{(1)}$	0.23	0.05	-0.00	0.28	0.23	0.03	-0.00	0.26	
$a_{\pi\Sigma}^{(0)}$	0.46	0.10	0.04	0.61	0.46	0.10	0.04	0.60	
$a_{\pi\Sigma}^{(3/2)}$	-0.12	0.04	-0.09	-0.17	-0.12	0.04	-0.09	-0.17	
$a_{\pi\Sigma}^{(1/2)}$	0.23	0.04	-0.03	0.24	0.23	0.04	-0.03	0.23	
$a_{\pi\Lambda}$	0.00	0.04	-0.11	-0.07	0.00	0.04	-0.11	-0.07	

* The scattering lengths are calculated from threshold T-matrices in Ref. [15].

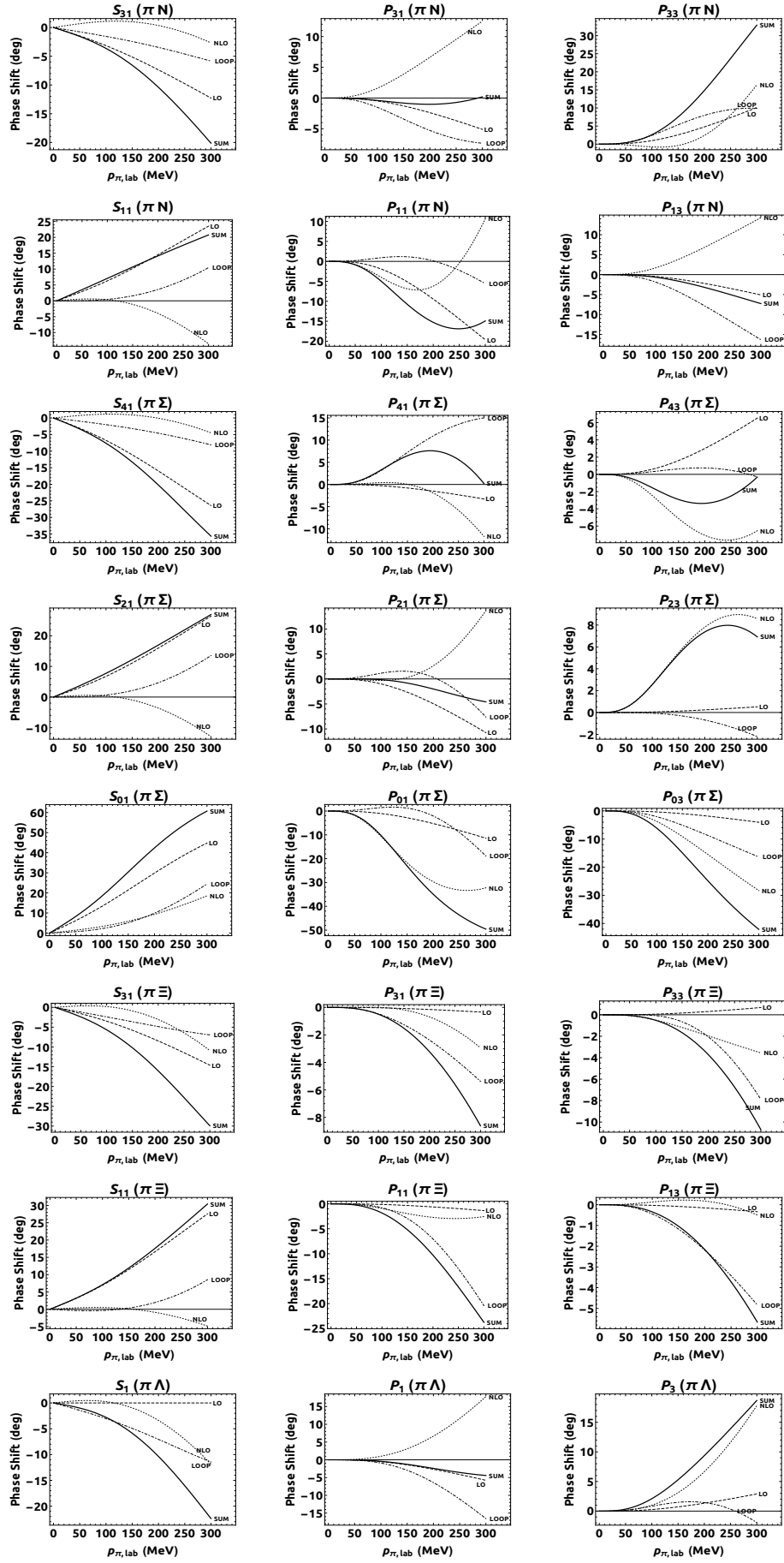


Figure 5: Predictions for the pion-baryon phase shifts versus the pion laboratory momentum. The dashed, dotted, dashed-dotted and solid lines denote the first-, second-, third-order and their sum contributions, respectively.

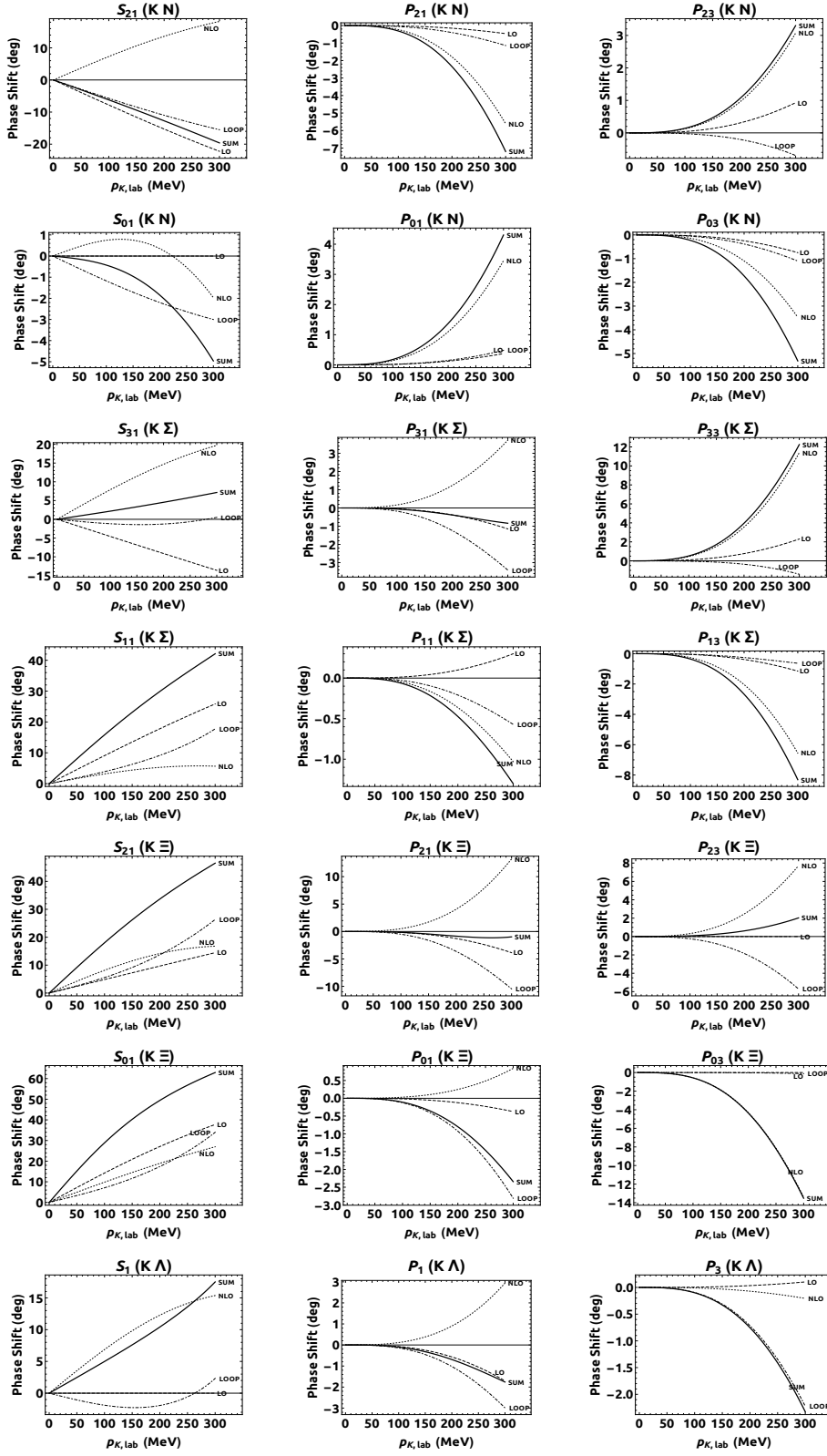


Figure 6: Predictions for the kaon-baryon phase shifts versus the kaon laboratory momentum. The notation for lines is the same as in Fig. 5.

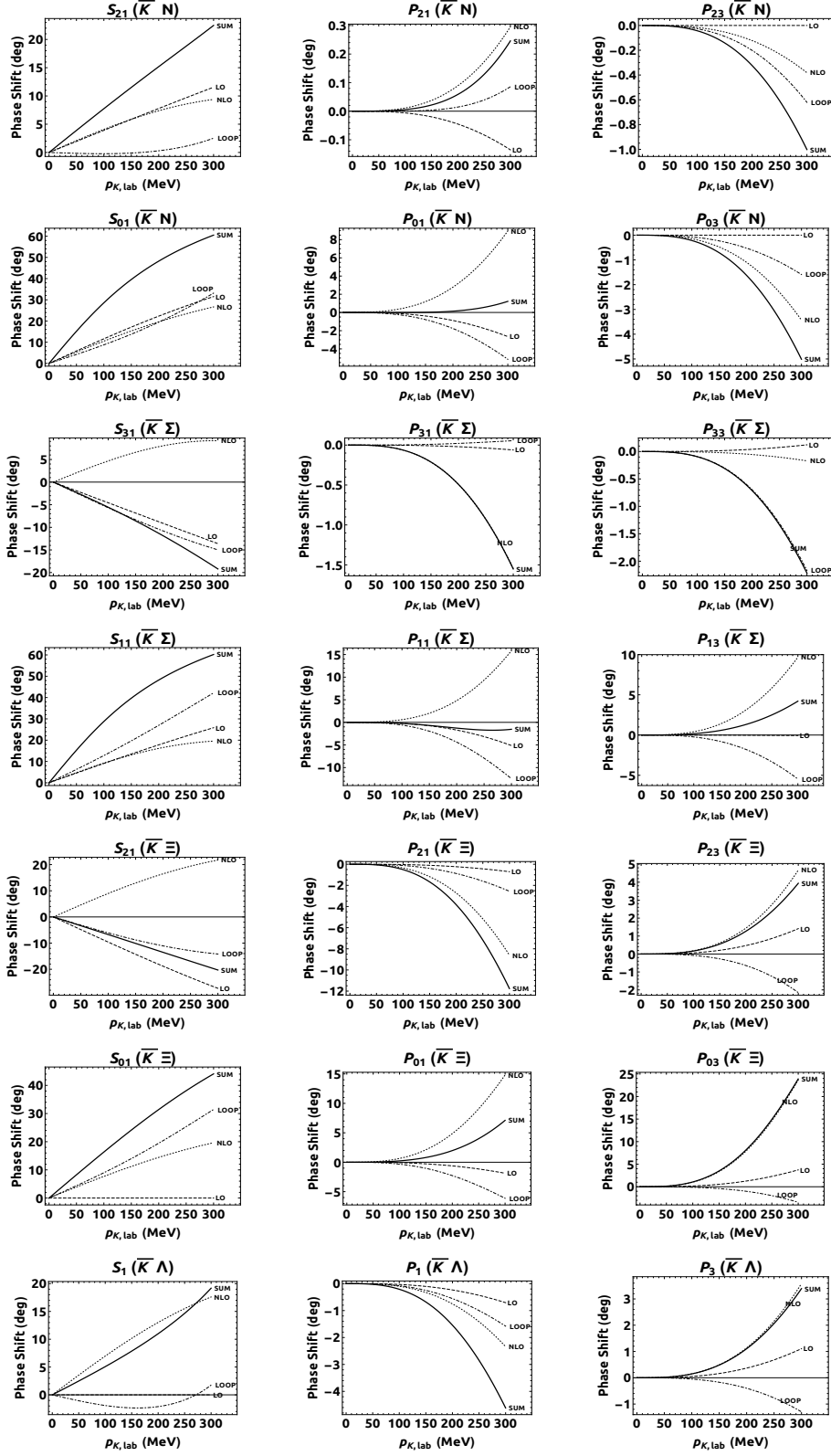


Figure 7: Predictions for the antikaon-baryon phase shifts versus the antikaon laboratory momentum. The notation for lines is the same as in Fig. 5.

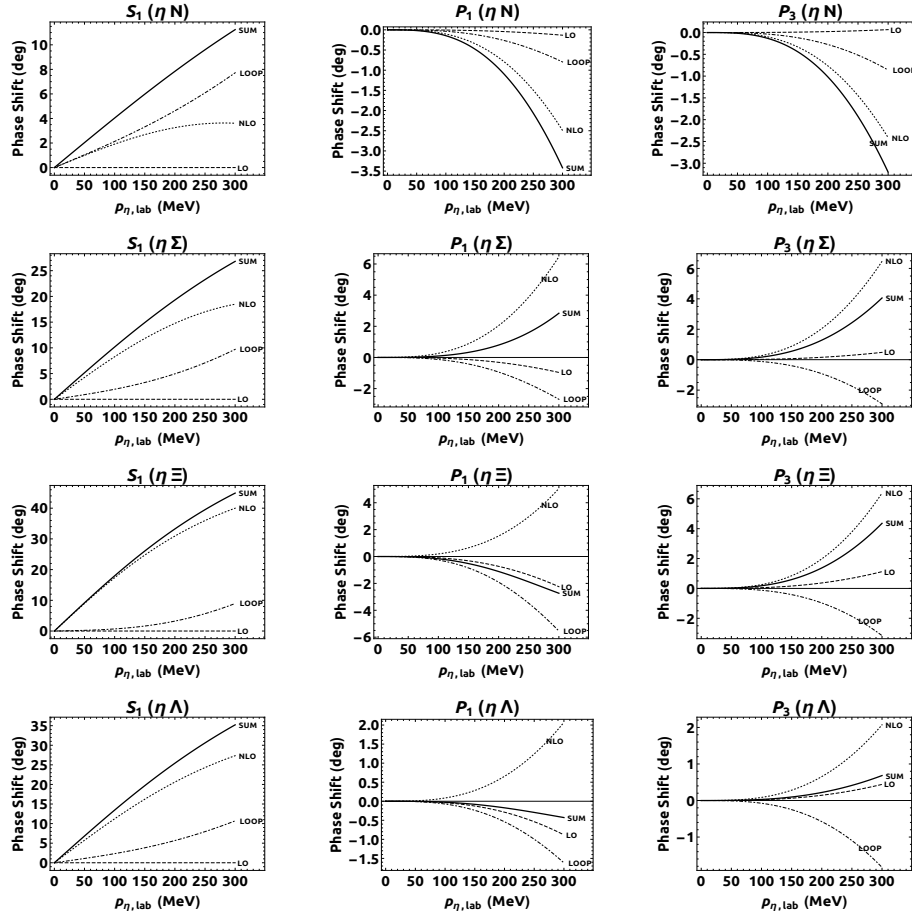


Figure 8: Predictions for the eta-baryon phase shifts versus the eta laboratory momentum. The notation for lines is the same as in Fig. 5.

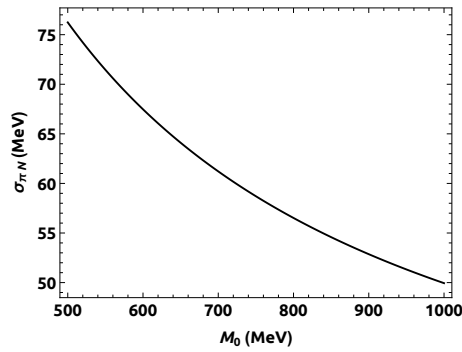


Figure 9: Relation between M_0 and $\sigma_{\pi N}$.

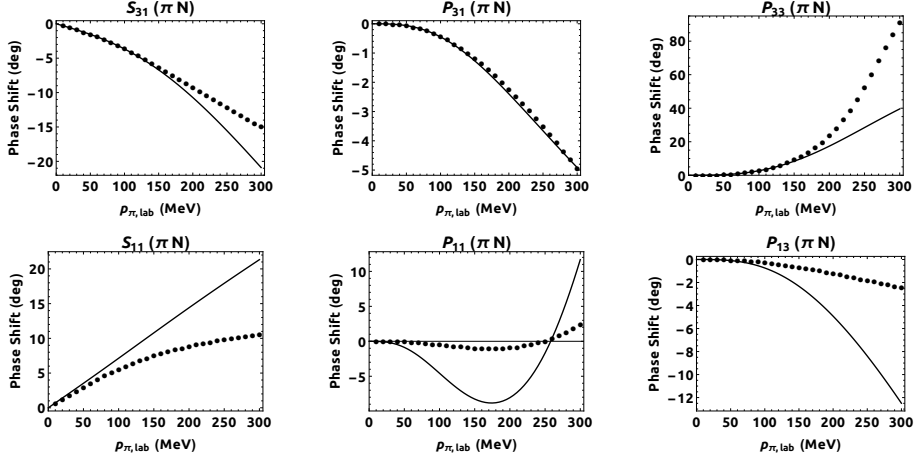


Figure 10: Fits and predictions for the WI08 phase shifts in πN scatterings versus the pion laboratory momentum. The notation is the same as in Fig. 3.

Table 2: Values of kaon-baryon scattering lengths from our calculations in comparison to the results of Liu [15]. The scattering lengths are in units of fm.

Our Prediction	$\mathcal{O}(q)$	$\mathcal{O}(q^2)$	$\mathcal{O}(q^3)$	Total	Liu*	$\mathcal{O}(q)$	$\mathcal{O}(q^2)$	$\mathcal{O}(q^3)$	Total
$a_{KN}^{(1)}$	-0.41	0.39	-0.31	-0.32	-0.40	0.35	-0.28	-0.33	
$a_{KN}^{(0)}$	0.00	0.05	-0.06	-0.01	0.00	0.08	-0.06	0.02	
$\text{Re } a_{K\Sigma}^{(3/2)}$	-0.22	0.39	-0.07	0.10	-0.21	0.27	-0.06	0.00	
$\text{Re } a_{K\Sigma}^{(1/2)}$	0.45	0.16	0.18	0.79	0.43	0.21	0.17	0.81	
$\text{Re } a_{K\Xi}^{(1)}$	0.23	0.40	0.24	0.87	0.22	0.28	0.24	0.74	
$\text{Re } a_{K\Xi}^{(0)}$	0.69	0.47	0.31	1.47	0.66	0.50	0.30	1.46	
$a_{K\Lambda}$	0.00	0.35	-0.11	0.25	0.00	0.27	-0.10	0.17	

* The scattering lengths are calculated from threshold T-matrices in Ref. [15].

Table 3: Values of antikaon-baryon scattering lengths from our calculations in comparison to the results of Liu [15]. The scattering lengths are in units of fm.

Our Prediction	$\mathcal{O}(q)$	$\mathcal{O}(q^2)$	$\mathcal{O}(q^3)$	Total	Liu*	$\mathcal{O}(q)$	$\mathcal{O}(q^2)$	$\mathcal{O}(q^3)$	Total
$\text{Re } a_{\overline{K}N}^{(1)}$	0.21	0.22	-0.02	0.41	0.20	0.22	-0.02	0.40	
$\text{Re } a_{\overline{K}N}^{(0)}$	0.62	0.57	0.44	1.63	0.60	0.49	0.42	1.50	
$\text{Re } a_{\overline{K}\Sigma}^{(3/2)}$	-0.22	0.24	-0.28	-0.26	-0.21	0.23	-0.26	-0.24	
$\text{Re } a_{\overline{K}\Sigma}^{(1/2)}$	0.45	0.47	0.61	1.52	0.43	0.29	0.57	1.30	
$a_{\overline{K}\Xi}^{(1)}$	-0.46	0.44	-0.30	-0.32	-0.44	0.39	-0.27	-0.32	
$a_{\overline{K}\Xi}^{(0)}$	0.00	0.37	0.41	0.78	0.00	0.17	0.39	0.57	
$a_{\overline{K}\Lambda}$	0.00	0.35	-0.11	0.25	0.00	0.27	-0.10	0.17	

* The scattering lengths are calculated from threshold T-matrices in Ref. [15].

Table 4: Values of eta-baryon scattering lengths from our calculations in comparison to the results of Liu [15]. The scattering lengths are in units of fm.

Our Prediction	$\mathcal{O}(q)$	$\mathcal{O}(q^2)$	$\mathcal{O}(q^3)$	Total	Liu*	$\mathcal{O}(q)$	$\mathcal{O}(q^2)$	$\mathcal{O}(q^3)$	Total
Re $a_{\eta N}$	0.00	0.11	0.11	0.22		0.00	0.06	0.12	0.18
Re $a_{\eta\Sigma}$	0.00	0.43	0.09	0.52		0.00	0.32	0.11	0.42
Re $a_{\eta\Xi}$	0.00	0.89	0.02	0.90		0.00	0.62	0.04	0.66
Re $a_{\eta\Lambda}$	0.00	0.59	0.11	0.70		0.00	0.56	0.13	0.69

* The scattering lengths are calculated from threshold T-matrices in Ref. [15].

Table 5: Predictions for the nucleon σ -term $\sigma_{\pi N}$ at the different values of the baryon mass M_0 in the chiral limit. Note that M_0 , α_N , B_π , $\sigma_{\pi N}$ are in units of MeV, and C_1 , C_2 , C_3 in units of GeV^{-1} .

M_0	α_N	B_π	C_1	C_2	C_3	$\chi^2/\text{d.o.f}$	$\sigma_{\pi N}$
751 ^a	-626.79	-47.70	-10.08	8.83	5.56	0.98	58.7
882 ^b	-622.94	-45.10	-10.06	8.90	5.56	0.98	53.5
880 ^c	-622.99	-45.13	-10.06	8.90	5.56	0.98	53.5
741	-627.14	-47.94	-10.08	8.82	5.56	0.98	59.1 ^d

^a M_0 is from a linear extrapolation to zero quark masses of lattice QCD results from Ref. [45].

^b M_0 from the Table I of Ref. [46] corresponding to $\sigma_{\pi N} = (49 \pm 3)$ MeV.

^c M_0 from the N^3LO result of Ref. [48] corresponding to $\sigma_{\pi N} = (55 \pm 5)$ MeV. .

^d $\sigma_{\pi N}$ has the same with the value of Ref. [49].

Acknowledgements

This work is supported in part by China Scholarship Council (CSC), the National Natural Science Foundation of China under Grants No. 11465021 and No. 11065010. B.-L.H. thanks Yan-Rui Liu (Shandong University) for very helpful discussions.

A Loop functions

In this appendix we present the basic loop-functions.

$$J_0(w, m) = \frac{1}{i} \int \frac{d^D l}{(2\pi)^D} \frac{1}{(v \cdot l - w)(m^2 - l^2)} = \frac{w}{8\pi^2} \left(1 - 2\ln \frac{m}{\lambda}\right) + \begin{cases} \frac{1}{4\pi^2} \sqrt{w^2 - m^2} \ln \frac{-w + \sqrt{w^2 - m^2}}{m} & (w < -m), \\ -\frac{1}{4\pi^2} \sqrt{m^2 - w^2} \arccos \frac{-w}{m} & (-m < w < m), \\ \frac{1}{4\pi^2} \sqrt{w^2 - m^2} \left(i\pi - \ln \frac{w + \sqrt{w^2 - m^2}}{m}\right) & (w > m), \end{cases} \quad (\text{A.1})$$

$$\frac{1}{i} \int \frac{d^D l}{(2\pi)^D} \frac{\{1, l^\mu, l^\mu l^\nu\}}{(m^2 - l^2)[m^2 - (l - k)^2]} = \{I_0(t, m), \frac{k^\mu}{2} I_0(t, m), g^{\mu\nu} I_2(t, m) + k^\mu k^\nu I_3(t, m)\}, \quad (\text{A.2})$$

$$I_0(t, m) = \frac{1}{8\pi^2} \left\{ \frac{1}{2} - \ln \frac{m}{\lambda} - \sqrt{1 - \frac{4m^2}{t}} \ln \frac{\sqrt{4m^2 - t} + \sqrt{-t}}{2m} \right\}, \quad (\text{A.3})$$

$$I_2(t, m) = \frac{1}{48\pi^2} \left\{ 2m^2 - \frac{5t}{12} + \left(\frac{t}{2} - 3m^2\right) \ln \frac{m}{\lambda} - \frac{(4m^2 - t)^{3/2}}{2\sqrt{-t}} \ln \frac{\sqrt{4m^2 - t} + \sqrt{-t}}{2m} \right\}, \quad (\text{A.4})$$

$$I_3(t, m) = \frac{1}{24\pi^2} \left\{ \frac{7}{12} - \frac{m^2}{t} - \ln \frac{m}{\lambda} - \left(1 - \frac{m^2}{t}\right) \sqrt{1 - \frac{4m^2}{t}} \ln \frac{\sqrt{4m^2 - t} + \sqrt{-t}}{2m} \right\}, \quad (\text{A.5})$$

$$H_0(t, m_1, m_2) = \frac{1}{i} \int \frac{d^D l}{(2\pi)^D} \frac{1}{v \cdot l (m_1^2 - l^2) [m_2^2 - (l - k)^2]} = \frac{1}{8\pi\sqrt{-t}} \arctan \frac{\sqrt{-t}}{m_1 + m_2}, \quad (\text{A.6})$$

where $t = k \cdot k < 0$. Note that terms proportional to the divergent constant $\lambda^{D-4} [\frac{1}{D-4} + \frac{1}{2}(\gamma_E - 1 - \ln 4\pi)]$ have been dropped.

The explicit analytical expression for the loop contributions of order $\mathcal{O}(q^3)$ to the meson-baryon scattering amplitudes can be obtained from the first author upon request.

References

- [1] S. Weinberg, *Physica*, **A96**, 327 (1979).
- [2] S. Scherer and M. R. Schindler, *Lect. Notes Phys.*, **830**, pp.1 (2012).
- [3] E. E. Jenkins and A. V. Manohar, *Phys. Lett.*, **B255**, 558 (1991).
- [4] V. Bernard, N. Kaiser, J. Kambor, and U. G. Meissner, *Nucl. Phys.*, **B388**, 315 (1992).
- [5] T. Becher and H. Leutwyler, *Eur. Phys. J.*, **C9**, 643 (1999).
- [6] J. Gegelia and G. Japaridze, *Phys. Rev.*, **D60**, 114038 (1999).
- [7] T. Fuchs, J. Gegelia, G. Japaridze, and S. Scherer, *Phys. Rev.*, **D68**, 056005 (2003).
- [8] X. L. Ren, L. S. Geng, J. Martin Camalich, J. Meng, and H. Toki, *JHEP*, **12**, 073 (2012).
- [9] J. M. Alarcon, J. Martin Camalich, and J. A. Oller, *Annals Phys.*, **336**, 413 (2013).

- [10] N. Fettes, U.-G. Meissner, and S. Steininger, Nucl. Phys., **A640**, 199 (1998).
- [11] N. Fettes and U.-G. Meissner, Nucl. Phys., **A676**, 311 (2000).
- [12] H. Krebs, A. Gasparyan, and E. Epelbaum, Phys. Rev., **C85**, 054006 (2012).
- [13] D. R. Entem, N. Kaiser, R. Machleidt, and Y. Nosyk, Phys. Rev., **C91**, 014002 (2015).
- [14] N. Kaiser, Phys. Rev., **C64**, 045204 (2001), [Erratum: Phys. Rev.C73,069902(2006)].
- [15] Y.-R. Liu and S.-L. Zhu, Phys. Rev., **D75**, 034003 (2007).
- [16] Y.-R. Liu and S.-L. Zhu, Eur. Phys. J., **C52**, 177 (2007).
- [17] Z.-W. Liu, Y.-R. Liu, and S.-L. Zhu, Phys. Rev., **D83**, 034004 (2011).
- [18] Z.-W. Liu and S.-L. Zhu, Phys. Rev., **D86**, 034009 (2012), [Erratum: Phys. Rev.D93,no.1,019901(2016)].
- [19] B.-L. Huang and Y.-D. Li, Phys. Rev., **D92**, 114033 (2015), [Erratum: Phys. Rev.D95,019903(2017)].
- [20] B. Borasoy and U.-G. Meissner, Annals Phys., **254**, 192 (1997).
- [21] B. Borasoy, Phys. Rev., **D59**, 054021 (1999).
- [22] J. A. Oller, M. Verbeni, and J. Prades, JHEP, **09**, 079 (2006).
- [23] V. Bernard, N. Kaiser, and U. G. Meissner, Phys. Lett., **B309**, 421 (1993).
- [24] V. Bernard, N. Kaiser, and U. G. Meissner, Phys. Rev., **C52**, 2185 (1995).
- [25] G. 't Hooft and M. J. G. Veltman, Nucl. Phys., **B153**, 365 (1979).
- [26] V. Bernard, N. Kaiser, and U.-G. Meissner, Int. J. Mod. Phys., **E4**, 193 (1995).
- [27] M. Mojziz, Eur. Phys. J., **C2**, 181 (1998).
- [28] A. O. Bouzas, Eur. Phys. J., **C12**, 643 (2000).
- [29] A. O. Bouzas and R. Flores-Mendieta, J. Phys., **G28**, 1179 (2002).
- [30] J. Gasser and U. G. Meissner, Phys. Lett., **B258**, 219 (1991).
- [31] T. E. O. Ericson and W. Weise, *Pions and Nuclei* (Clarendon Press, Oxford, UK, 1988).
- [32] K. A. Olive *et al.* (Particle Data Group), Chin. Phys., **C38**, 090001 (2014).
- [33] R. L. Workman, R. A. Arndt, W. J. Briscoe, M. W. Paris, and I. I. Strakovsky, Phys. Rev., **C86**, 035202 (2012).
- [34] J. S. Hyslop, R. A. Arndt, L. D. Roper, and R. L. Workman, Phys. Rev., **D46**, 961 (1992).
- [35] W. J. Briscoe *et al.*, SAID on-line program, see <http://gwdac.phys.gwu.edu>.
- [36] J. Dobaczewski, W. Nazarewicz, and P. G. Reinhard, J. Phys., **G41**, 074001 (2014).
- [37] B. D. Carlsson, A. Ekström, C. Forssén, D. F. Strömberg, G. R. Jansen, O. Lilja, M. Lindby, B. A. Mattsson, and K. A. Wendt, Phys. Rev., **X6**, 011019 (2016).
- [38] J. Caro Ramon, N. Kaiser, S. Wetzel, and W. Weise, Nucl. Phys., **A672**, 249 (2000).
- [39] N. Kaiser, T. Waas, and W. Weise, Nucl. Phys., **A612**, 297 (1997).
- [40] N. Kaiser, P. B. Siegel, and W. Weise, Nucl. Phys., **A594**, 325 (1995).
- [41] E. Oset and A. Ramos, Nucl. Phys., **A635**, 99 (1998).
- [42] J. A. Oller and U. G. Meissner, Phys. Lett., **B500**, 263 (2001).
- [43] M. F. M. Lutz and E. E. Kolomeitsev, Nucl. Phys., **A700**, 193 (2002).
- [44] T. Hyodo and D. Jido, Prog. Part. Nucl. Phys., **67**, 55 (2012).
- [45] Y. Kuramashi, M. Fukugita, H. Mino, M. Okawa, and A. Ukawa, Phys. Rev. Lett., **72**, 3448 (1994).
- [46] M. Procura, B. U. Musch, T. Wollenweber, T. R. Hemmert, and W. Weise, Phys. Rev., **D73**, 114510 (2006).
- [47] X.-L. Ren, L.-S. Geng, and J. Meng, Eur. Phys. J., **C74**, 2754 (2014).
- [48] X.-L. Ren, L.-S. Geng, and J. Meng, *Proceedings, 8th International Workshop on Chiral Dynamics (CD15): Pisa, Italy, June 29-July 3, 2015*, PoS, **CD15**, 085 (2016).
- [49] M. Hoferichter, J. Ruiz de Elvira, B. Kubis, and U.-G. Meißner, Phys. Rev. Lett., **115**, 092301 (2015).